Vane Tip Detachment in a Positive Displacement Vane Pump

Myung-Rae Cho* and Dong-Chul Han**

(*Received December 17, 1997*)

This paper reports on the theoretical study of the transient chamber pressure and vane motion in a positive displacement vane pump which widely used in the automotive power steering systems. For analyzing the vane detachment, dynamic equation of vane motion and flow continuity equations are derived and then solved simultaneously using the numerical integration. Vane detachment is shown to be a function of the chamber pressure, rotational speed, and the design geometry of pump. Vane detachment occurs due to excess compression of chamber volume, and it can be reduced by adjustment of design parameters. Specially, silencing V-groove in side plate and radius reduction ratio of compression zone in the cam ring are important design factors for reducing the vane detachment.

Key Words: Positive Displacement Vane Pump, Vane Detachment, V-groove, Radius reduction ratio.

Nomenclature

A : Orifice area at x_1
$a(x)$: Groove orifice area at x
B_e : Bulk modulus of fluid
b_v : Width of vane
C : Orifice flow coefficient
c_c : Damping coefficient of cam ring
F_{b1} : Top reaction force exerted at the top of the rotor slot
F_{b2} : Bottom reaction force exerted at the vane bottom within rotor slot
F_{c1} : Downstream vane tip force
F_{c2} : Upstream vane tip force
F_{co} : Coriolis force
F_i : Inertia force
F_o : Reaction force cam/vane tip interface
F_{pd} : Leading vane chamber pressure force
F_{pp} : Trailing vane chamber pressure force
F_{uvp} : Under vane force
F_{vr} : Friction force between vane and rotor slot in Y-axis
F_{vs} : Friction force between vane and side plate in Y-axis
$F_{v\omega}$: Friction force between vane and side plate in rotational direction
h_v : Height of vane
k_c : Stiffness coefficient of cam ring
l_1 : $R_v - r_r$
l_2 : $R_v - r_{uvp}$
m_v : Mass of vane
P : Pumping chamber pressure
P_d : Discharge pressure
Q_d : Outlet flow from the chamber
Q_l : Total leakage flow
Q_{l1} : Vane side leakage
Q_{l2} : Vane tip leakage
Q_{l3} : Rotor slot leakage
Q_{l4} : Rotor side leakage
Q_s : Inlet flow to the chamber
$R.R.R.$: Radius reduction ratio
R_v : Vane tip radius from the rotor center
r_c : Radius of cam ring
r_r : Radius of rotor
r_{uvp} : Radius of under vane port
t_v : Thickness of vane

* Graduate School, Seoul National University
** Department of Mechanical Design & Production Engineering, Seoul National University

U : Radial velocity of vane $\left(-\omega\frac{dR_v}{d\theta}\right)$
V : Pumping chamber volume
X, Y : Coordinate system
x_1 : Position of the vane
x_2 : Position of th e end of the fluid jet
z : Number of vane
α : $\frac{|U|}{U}$
β : $\frac{|F_{pd}-F_{pp}|}{F_{pd}-F_{pp}}$
δ_{max} : Maximum vane detachment
μ_r, μ_t : Friction coefficient
θ_v : Depth angle of silencing groove
θ_h : Horizontal angle of silencing groove
ρ : Density of working fluid
ω : Angular speed

1. Introduction

Positive displacement vane pumps are widely used as a hydraulic sources in the automotive power steering systems due to structural simplicity, higher power in spite of small size and low weight and economical superiority in comparison with variable displacement vane pumps and piston pumps. Vane pumps have several moving parts, therefore sufficient clearances between moving parts have to be maintained for smooth operations. But these clearances are paths of leakage flow, and pressure fluctuations and noise are caused by fluctuations in leakage flows and vibrations from moving elements (Ueno, H., et al., 1989; Seet, G. G. L., et al., 1990).

Generally, vanes have to move with sufficient gap between vane and cam surface. However, if insufficient forces are acting on the vanes, vane detachments at the cam surface can occur. When this occurs, firstly, the vane motion shows an oscillation between contact and non-contact with cam ring. Secondly, it causes the noise according to re-attachment of vane. Finally, this phenomenon increases wears of vane and cam surface. Therefor, maintaining the proper contact between cam surface and vane is the most important design criterion. Watton (1990) and Karmel (1986a, 1986b) have been investigated the transient pressure characteristics and dynamics of vane, but relationship of vane motion and excess chamber pressure was not discussed. Although Edge et al. (1986) and Dickinson et al. (1993) have presented the models for dynamics of vane motions and pressure fluctuations, results of analysis were not shown. Nishiumi et al. (1993) have studied vane detachment theoretically and experimentally of variable displacement vane pump. To the authors' knowledge, analysis of vane detachment and parametric study have not been reported for the positive displacement vane pumps. So, this paper investigated analytically the relations of transient chamber pressure and vane motion, and their dependence on the design and operating parameters.

2. Description of Pumping Cycle

Figure 1 displays a schematic diagram of a positive displacement vane pump analyzed in this paper. The pump consists of the cam ring, rotor, vanes and plates. Figure 2 shows the configuration of cam ring profile. The cam ring curve is composed of four region. Region A is a constant radius zone. As the rotor advances, working fluid is drawn through the suction ports in region B, and then compression chamber reaches the end of suction ports and enters pre-compression area in region C. The cam curve in region B is constructed by using fifth degree of polynomial and used Archimedes curve in region C. In the compression

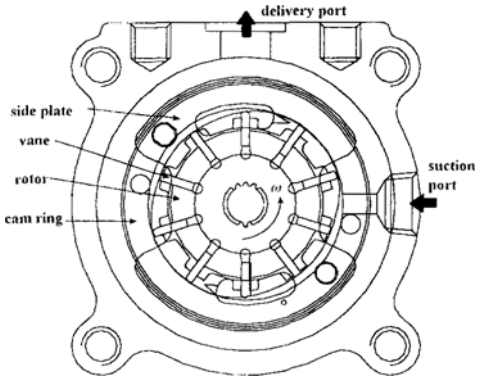

Fig. 1 Schematic diagram of positive displacement vane pump.

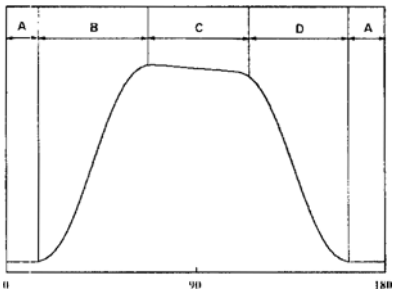

Fig. 2 Configuration of cam profile.

zone, chamber pressure rises according to a decreass in chamber volume. If this pressure does not match the delivery pressure when pumping chamber opens to the delivery ports, flow pulse is generated, lasting until the pressure equalize (Dickinson, K. A., et al., 1993). Therefore, in region C, the cam ring radius is decreasing with increasing the angular position. Then, fluid is compressed to, ideally, match the load pressure at the delivery ports in region D, but this can only be obtained at a given operating condition, such as fixed load pressure and rotational speed. So, if excess compression occurs in this region, chamber pressure rises over the load pressure so called pressure overshoot, and then it causes the vane jumping phenomenon from the cam surface. This pressure overshoot and vane detachment can be controlled by combination of silencing V-groove in side plate and radius reduction ratio in region C

3. Pressure Analysis

This section describes fundamental equations used in the chamber pressure analysis. Figure 3 shows cross section of pumping chamber. The control volume used in the simulation consists of cam ring, rotor and a pair of vanes. In this paper, only one chamber is considered.

Applying the continuity equation to the control volume, we have governing equation for chamber pressure given by

$$\frac{dP}{dt}=\frac{B_e}{V}\left(-\frac{dV}{dt}+{}_d+Q_s+Q_l\right) \tag{1}$$

In Eq. (1), inlet and outlet flows Q_s and Q_d are

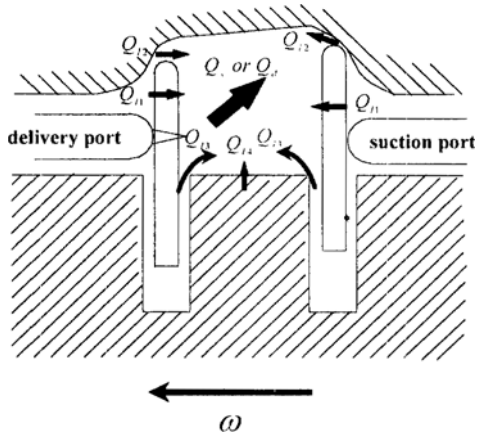

Fig. 3 Schematic diagram of pumping chamber.

determined using the orifice equation. Q_l is total leakage flow, where

$$Q_l=Q_{l1}+Q_{l2}+Q_{l3}+Q_{l4} \tag{2}$$

In addition to Eq. (1), we consider the effects of fluid inertia. Edge(1986) found that pressure oscillations within the piston pump's port plate metering groove and silencing V-groove in vane pump's side plate were affected by fluid inertia. To consider this phenomenon, Edge's analysis has been used in this study. The differential equation for fluid inertia effect through the silencing V-groove is

$$\Delta P=\frac{\rho}{2}\left(\frac{Q}{CA_1}\right)^2 sgn(Q)+\rho\omega\frac{dQ}{d\theta}\int_{x_1}^{x_2}\frac{dx}{a(x)} \tag{3}$$

More detailed explanations, refer to references (Edge, K. A., et al., 1986; Dickinson, A. L., et al., 1993). The solution to Eq. (1) through Eq. (3) is obtained by numerical integration and yields the chamber pressure. The pressure will thus be expressed in terms of angular position, and it is a function of the design geometry and operating conditions of the pump.

4. Vane Detachment Analysis

Figure 4 shows dynamic forces acting on the vane. To formulate a set of dynamic equations of vane motion, following assumptions are made.

- Constant rotational speed.
- Under vane pressure is constant as delivery

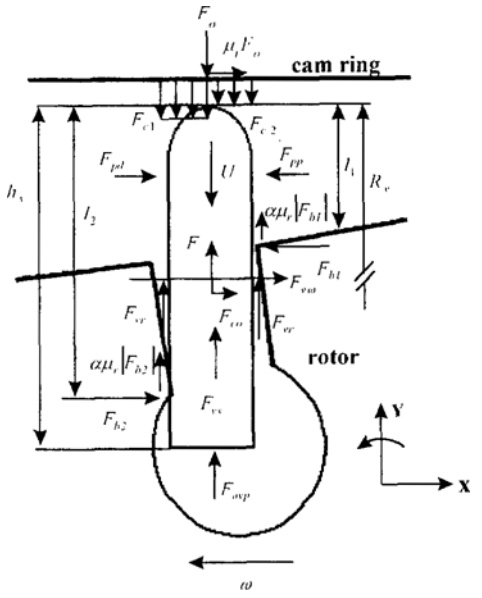

Fig. 4 Schematic diagram of vane force.

pressure.

- Constant clearances between moving parts.
- Pressure acting on each side of the vane tip are equal to each chamber pressure
- Negligible deflections and vibrations of elements.
- Inclination of the cam surface relative to the vane is negligible.
- Negligible moment contribution from vane -slot friction force.

Tangential force balance, radial force balance and moment balance about the vane tip are as follows:

$$F_{pd}-F_{pp}+F_{b2}-F_{b1}+\mu_t F_o+2F_{vw}+F_{co}=0 \quad (4)$$

$$\frac{1}{2}h_v F_{co}+\frac{1}{2}l_1(F_{pd}-F_{pp})+2(R_v-r_{vw})F_{vw}+l_2F_{tr}-l_1F_{b1}+\frac{1}{2}\alpha\mu_r t_v(F_{b1}-F_{b2})+\frac{1}{4}t_v(F_{c1}-F_{c2})=0 \quad (5)$$

$$F_i+2(F_{vr}+F_{vs})+(F_{uvp}-F_{c1}-F_{c2})+\alpha\beta\mu_r(F_{b1}+F_{b2})-F_o=0 \quad (6)$$

In Eq. (6), F_o is the force exerted between cam ring surface and vane tip. It is defined as

$$F_o=0 \quad (R_v<r_c)$$

$$F_o=k_c(R_v-r_c)+c_c\dot{R}_v \quad (R_v\geq r_c) \quad (7)$$

Arranging Eq. (4) through Eq. (6), we obtain the dynamic equation of vane motion as follows:

$$\frac{d^2R_v}{d\theta^2}=R_v-\frac{h_v}{2}+\frac{F_{y1}+F_{y2}+F_{y3}}{m_v\omega} \quad (8)$$

where,

$$F_{y1}=F_{uvp}-F_{c1}-F_{c2}-F_o$$
$$F_{y2}=2(F_{vr}+F_{vs}) \quad (9)$$
$$F_{y3}=\alpha\beta\mu_r(F_{b1}+F_{b2})$$

As the sets of the Eq. (1), Eq. (3) and Eq. (8) are solved simultaneously by using the 4th order Runge-Kutta method, we can obtain the chamber pressure and vane locus in terms of angular position.

5. Results

Table 1 shows the specification of test vane pump and property of working fluid. Figure 5 shows an example of vane detachment and transient chamber pressure. Pumping chamber pressure and vane locus are displayed with angular position θ for two types radius reduction ratio. They show peak pressure and pressure oscillations in the silencing groove zone. Figure 5(a) shows higher peak pressure than Fig. 5(b) in silencing groove zone The vane detachment hap-

Table 1 Specification of test vane pump and property of working fluid.

Element	Dimension
Radius of rotor	15.6mm
Radius of small arc	18.0mm
Radius of large arc	19.5mm
Width of vane	5.0mm
Length of vane	7.0mm
Thickness of vane	1.6mm
Number of vane	10
Main operating condition	1500rpm, 6MPa
B_e	0.343GPa
ρ	850kg/m^3

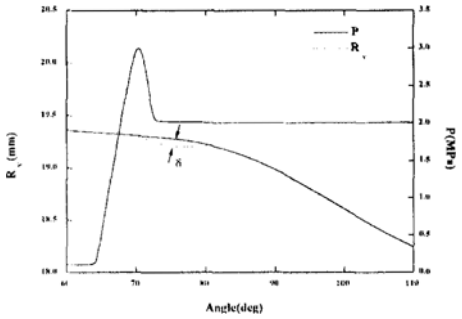

(a) R. R. R.=1%

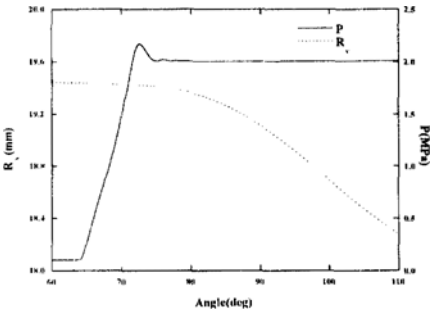

(b) R. R. R.=0.4%

Fig. 5 Pressure distribution and vane locus (ω=157.1 rad/s, P_d=2MPa, θ_h, θ_v:15°)

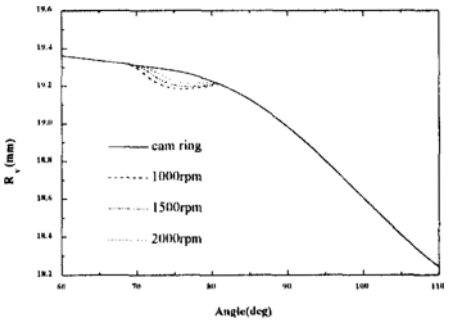

Fig. 6 Rotational speed effect on the vane locus (P_d =2MPa, R. R. R.=1%, θ_h, θ_v:15°).

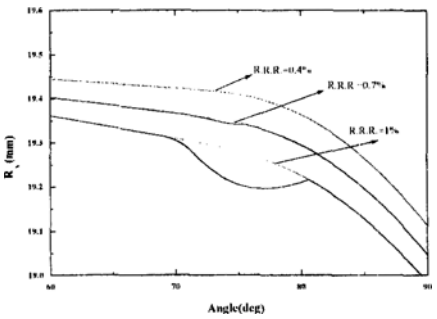

Fig. 7 Radius reduction ratio effect on the vane locus (ω=157.1 rad/s, P_d=2MPa, θ_h, θ_v: 15°).

pens in this region due to excess chamber pressure. Also, it is known that vane jumping starts at peak pressure point and continues after chamber pressure matched with load pressure.

Figure 6 shows an example of vane locus for the rotational speed variations. The effect of an increase in speed is to delay the vane detaching at any given rotational position and re-attachment angle is shortened. As rotational speed increases, vane detachment is decreased due to increasing inertia force.

Figure 7 shows the effects of radius reduction ratio on the vane locus. Three cases R. R. R. are used in this study. At higher R. R. R., vane detachment increases because of excess compression which is induced relatively large and rapid chamber volume decreasing rate. Therefore, for preventing the vane jumping phenomenon, it is necessary for radius reduction ratio to be well designed so that chamber pressure may accord ideally with load pressure.

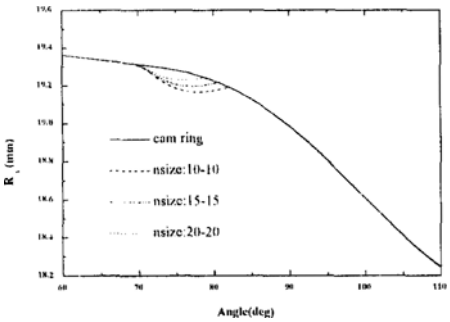

Fig. 8 Silencing groove size effect on the vane locus (ω=157.1 rad/s, P_d=2MPa).

An example of the effect of silencing groove size is shown in Fig. 8, where three cases are used. Amount of maximum vane detachment is increased as groove size decreases, because compression is continued until the delivery port is fully opened at small groove, and then chamber pressure becomes higher than large groove. So, vane detachment can be reduced by proper groove size

Table 2 Predicted δ_{max}(m) as function of delivery pressure and rotational speed for R. R. R.

RPM	R.R.R(%) P_d(MPa)	0.4	0.7	1.0
1000	1	1.689e-5	7.680e-5	1.293e-4
	2	0	4.612e-5	1.080e-4
	4	0	4.13e-7	3.998e-5
	6	0	0	9.315e-6
1500	1	2.935e-6	6.739e-5	1.227e-4
	2	0	2.768-5	9.644e-5
	4	0	0	2.907e-6
	6	0	0	7.99e-7
2000	1	0	5.313e-5	1.114e-4
	2	0	1.169e-5	8.126e-5
	4	0	0	1.504e-5
	6	0	0	0

(a) θ_h, $\theta_v=10°$

RPM	R.R.R(%) P_d(MPa)	0.4	0.7	1.0
1000	1	3.86e-6	7.096e-5	1.276e-4
	2	0	1.714e-5	9.168e-5
	4	0	0	1.172e-5
	6	0	0	1.054e-6
1500	1	0	5.513e-5	1.166e-4
	2	0	5.09e-5	7.371e-5
	4	0	0	2.601e-6
	6	0	0	0
2000	1	0	3.514e-5	9.914e-5
	2	0	0	5.314e-5
	4	0	0	0
	6	0	0	0

(b) θ_h, $\theta_v=15°$

RPM	R.R.R(%) P_d(MPa)	0.4	0.7	1.0
1000	1	0	6.397e-5	1.255e-4
	2	0	4.169e-6	7.313e-5
	4	0	0	2.305e-6
	6	0	0	2.9e-7
1500	1	0	4.256e-5	1.092e-4
	2	0	0	5.085e-5
	4	0	0	0
	6	0	0	0
1000	1	0	2.046e-5	8.543e-5
	2	0	0	2.935e-5
	4	0	0	0
	6	0	0	0

(c) θ_h, $\theta_v=20°$

selection.

Table 2 summarizes predicted amount of maximum vane detachment for **R. R. R.** and groove size variations at each operating condition. Three types **R. R. R.** and groove size were used in this study.

Amount of maximum vane detachment decreases as speed increases, because inertia force increases. This decreases as load pressure increases at each **R. R. R** and speed, because pre-compression by **R. R. R** is well matched with load pressure. At higher **R. R. R.**, maximum vane detachment increases due to the excess compression.

In the case of groove size test, vane detachment decreases as size increases all operating conditions. It is very effective to reduce the amount of vane detachment at lower **R. R. R** and higher load pressure.

Therefore in the case of this test pump, when radius reduction ratio is 0.4% and size angle of groove is 20°, it is operated smoothly without detachment under most of operating conditions. IF **R. R. R** is selected lower than 0.4% and groove size above 20°, vane jumping will not occur, but amount of pre-compression is a little or opening area of delivery port is relatively large, and thus chamber pressure will be affected by reverse flow from the delivery port. In these cases, delivery flow and pressure ripples may increase.

6. Conclusion

It is possible from the model developed initially by Dickinson et al. (1993) to evaluate the effect of the design parameters on the vane detachment in a positive displacement vane pump.

Vane locus plots and tables show that vane detachment occurs due to the excess compression of chamber volume, and it is a function of the design parameters and operating conditions; it reduces as rotational speed and load pressure increase at each design parameter, and decreasing in radius reduction ratio and increasing in silencing groove size at each operating condition. Specially, radius reduction ratio of the compression zone in cam ring is very effective to prevent the vane detachment from excess compression. Also groove size is effective in the case of lower R. R. R. and higher load pressure, but the effect of groove size is less than that of radius reduction ratio. It is thought that these trends will be maintained irrespective of pump capacity. If the capacity of pump is changed, the optimal values of design parameters can be selected by using the above procedures.

Therefore, these results may be used to prevent vane detachment and design cam ring and silencing groove for the hydraulic vane pumps. Also, experimental study will be required to verify the theoretical analysis.

Acknowledgments

This work was carried out at the Turbo & Power Machinery Research Center in Seoul National University as a part of G7 Project funded by Korean Government.

References

Dickinson, A. L., Edge, K. A., and Johnston, D. N., 1993, "Measurement and Prediction of Power Steering Vane Pump Fluidborne Noise," *SAE931294*, pp. 267~275.

Edge, K. A., and Daring, J. 1986, "Cylinder Pressure Transients in Oil Hydraulic Pumps with sliding Plate Valve," *Proc. I. Mech. Eng.* Vol. 200, No. B1, pp. 45~54.

Karmel, A. M., 1986, "A Study of the Internal Forces in a Variable-Displacement Vane Pump -Part I : A Theoretical Analysis," *ASME, J. of Fluids Eng.* Vol. 108, pp. 227~232.

Karmel, A. M., 1986, "A Study of the Internal Forces in a Variable-Displacement Vane Pump -Part II : A Parametric Study," *ASME, J. of Fluids Eng.* Vol. 108, pp. 233~237.

Nishiumi, T., and Maeda, T., 1993, "Motion of the Vane in a Variable Displacement Vane Pump -1st Report : On the Vane Jumping Phenomenon in the Process of Compression," *J. of the JHPS.*, Vol. 24, No. 2, pp. 105~112.

Seet, G. G. L., Penny, J. E. T., and Foster, K., 1990, "Applications of a Computer Model in the Design and Development of a uiet Vane Pump," *Proc. I. Mech. Eng.*, Vol. 199, No. B4, pp. 247~253.

Uneo, H., Shintani, R., and Okajima, 1989, "A Pressure and Flow Ripples of a Variable Displacement Vane-Pump," *First JHPS International Symposium on Fluid Power*, Tokyo, pp. 131~137.

Watton, J., and Watkins, K., 1990, "The Transient Pressure Characteristic of a Positive Displacement Vane Pump," *Proc. I. Mech. Eng.* Vol. 204, pp. 269~275.